Guo *et al.*
Chinese Journal of Mechanical Engineering (2022) 35:62
https://doi.org/10.1186/s10033-022-00709-0

Chinese Journal of Mechanical Engineering

ORIGINAL ARTICLE

Open Access

Study on the Distribution of Frictional Forces on *Z*-yarn Continuous Implanted Preforms and Their Applications

Zitong Guo[1,3], Zhongde Shan[2*], Jihua Huang[1] and Debo Xue[4]

Abstract

To improve the quality and efficiency of *Z*-directional 3D preform forming, the *Z*-yarn frictional force distribution model of the preform and its wear mechanism were investigated. In this study, a tensile force measuring device was designed to measure the force required to replace the guide sleeve, which is equivalent to the *Z*-yarn frictional forces. The frictional force is proportional to the number of preform layers and is applied to the preform decreased from the corner, edge, sub-edge, and middle in order. A back propagation neural network model was established to predict the friction at different positions of the preform with different layers, and the error was within 1.9%. The wear of *Z*-yarn was studied at different frictional positions and after different times of successive implantation into the preform. The results showed that with an increase in the number of *Z*-yarn implantations and frictional forces, the amount of carbon fiber bundle hairiness gradually increased, and the tensile fracture strength damage of the fiber was increasingly affected by the frictional forces. In the corner position of the preform, when the number of implantations was 25, the fiber fracture strength decreased non-linearly and substantially; in order to avoid fiber fracturing in the implantation process, the *Z*-yarn needs to be replaced in time after 20–25 cycles of continuous implantation. This study solves the problem of difficulty in measuring the force required for individual replacements owing to the excessive number of guide sleeves, puts forward the relationship between fiber wear, preform position, and implantation times, solves the phenomenon of fracture in the preform during *Z*-direction fiber implantation, and realizes the continuous implantation of fibers.

Keywords: *Z*-yarn implantation, BP neural network, *Z*-yarn wear

1 Introduction

Advanced composite materials are widely used in the fields of aerospace, defense, military, rail transportation, etc., and are contested by industrially developed countries as strategic must-have resources. C/C composites with excellent high-temperature performance are widely used in missile warheads, solid rocket engine nozzles, aircraft brake discs, space shuttle structural components, and other applications [1]. The carbon fiber preform is the most basic reinforcing structural body of C/C composites, and can determine the volume content of fibers and fiber orientation, influence the pore geometry, distribution of pores and the degree of fiber bending and twisting in the composites, and determine the performance of the composites. C/C composites have always been a major topic for research in the industry [2–4].

Three-dimensional (3D) preforms contain load-bearing fibers in all directions, solving the shortcomings of two-dimensional (2D) preforms, which had insufficient interlayer performance and were easy to damage. 3D preforms have better load-bearing performance, have received more attention. The application of the current needling process for complex fiber structures will lead to preform damage which is difficult to describe, and a

*Correspondence: shanzd@cam.com.cn

[2] Nanjing University of Aeronautics and Astronautics, Nanjing 210016, China
Full list of author information is available at the end of the article

large dispersion in macroscopic mechanical behavior [5]. 3D woven composites have complex structures, long process cycles, and are expensive to develop using traditional design methods [6]. Weaving of complex curved components is also a difficult task. The overall degree of automation of woven molded preforms is still not sufficient to meet the demands of short-time high-volume production [7], which restricts the development and application of 3D woven fabrics to a certain extent.

The digital 3D weaving and forming proposed by Shan et al. [8], as shown in Figure 1, used a layered weaving method with digital templates, which realized the weaving and formation of complex preforms by creating and forming structural parts along digitally guided templates with fibers under computer control. We used CAD to generate the model of the preform and arrange the guide sleeves to limit the shape of the preform. The forming process of the composite preform first lays the fiber bundles in the X and Y directions between the guide template layer by layer, uses the side bar and guide sleeve to restrain the shape of the fiber position, layers to a certain thickness for compaction densification, then repeats the previous steps to complete the weaving of the preform, as shown in Figure 2.

After weaving, the Z-yarn must be inserted into the preform to replace the guide sleeve, as shown in Figure 3. First, a steel needle (called a replacement needle) carrying the Z-yarn is used to position the needle at the coaxial point of the guide sleeve, as shown in Figure 3(a), and move forward along the guide sleeve to replace the guide sleeve while introducing the Z-yarn into the preform, as shown in Figure 3(b). After replacing the first guide sleeve, the second guide sleeve is replaced in the opposite direction, as shown in Figure 3(c), and the Z-yarn is implanted into the preform again as shown in Figure 3(d). The entire guide sleeve is repeatedly replaced with a replacement needle carrying the Z-yarn into the preform, finally forming a three-dimensional preform.

About research on Z-yarn, Hassan et al. [9] showed that the accurate design of the Z-yarn path and more importantly, its frequency in a three-dimensional woven structure is essential for impact-resistant composite structures. Midani et al. [10] found that changing the number of Z-yarns in the structure has a negligible effect on tensile strength (in-plane) and a significant effect on the weight reduction impact performance (out-of-plane). Esmaeeli et al. [11] used the finite element method to establish a composite cell model and found that the optimal out-of-plane elastic modulus largely depended on the Z-yarn distribution density and the ratio of yarn width to yarn radius. Bilisik [12] pointed out that the root cause of the structural instability of the preform was the thickness variation, where the main factors were the width ratio of the preform and the thickness variation, where the main factors are the width ratio of the preform and the introduction path of Z-yarn fibers. Xu et al. [13] pointed out that the interlayer intercut strength of 3D needled SiC increased with increasing yarn size and Z-yarn density, and decreased with Z-yarn density. Scholars have only pointed out the importance of Z-yarn for preforms and composites, but the distribution pattern of the frictional forces to which Z-yarn is implanted in preforms has not been studied.

Regarding friction studies of fibers, Eddine et al. [14] found that the transverse friction was relatively stable, and the friction coefficient was smaller than the longitudinal friction. Allaoui et al. [15] found that the relative orientation of the yarns in the fabric had a significant effect on the coefficient of friction, which increased with increasing warp and weft densities. Tourlonias et al. [16] found a decreasing trend in the coefficient of friction and its coefficient of variation for carbon fiber bundles as the degree of pulp film wear between the filaments increased. Cornelissen et al. [17] explored the relationship between carbon fiber bundles and the friction properties of fabrics at three scales (microscopic, fine, and macroscopic) to predict the friction pattern between satin fabrics woven

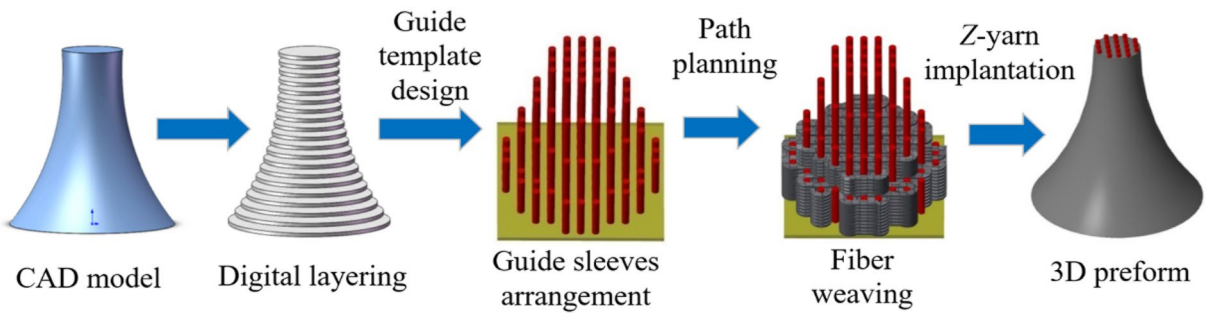

Figure 1 Digital weaving forming

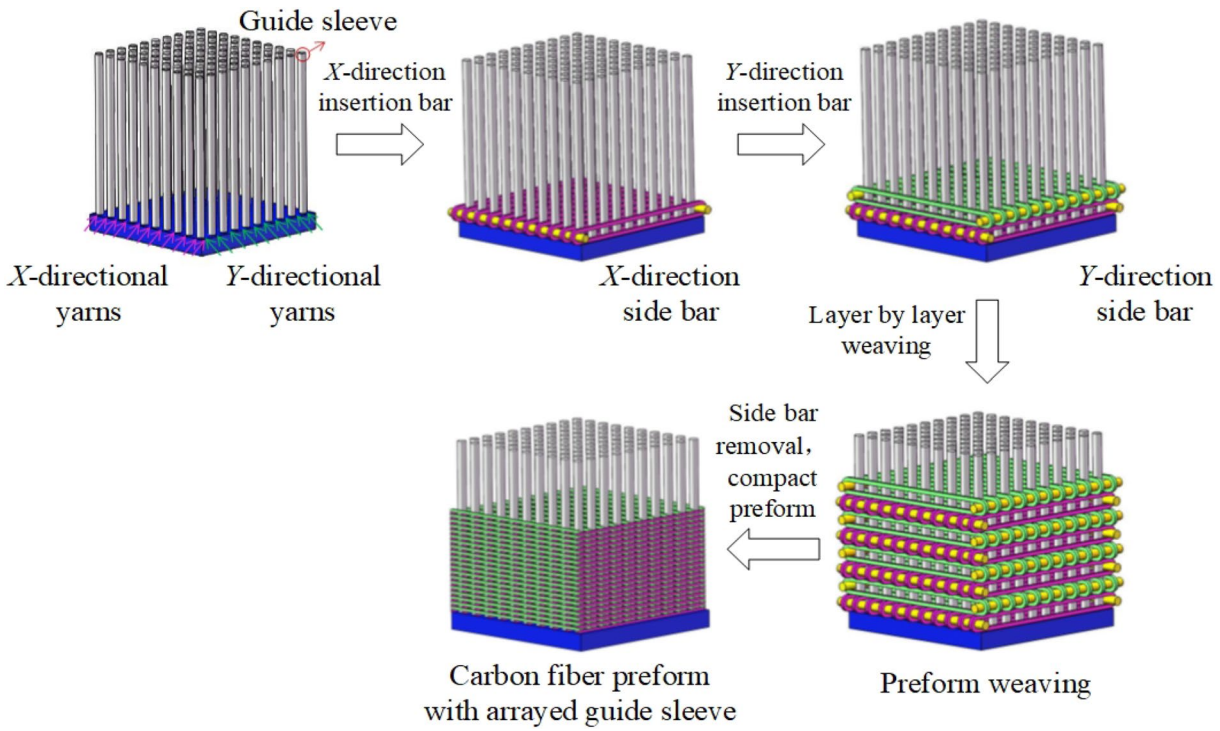

Figure 2 Composite preform weaving

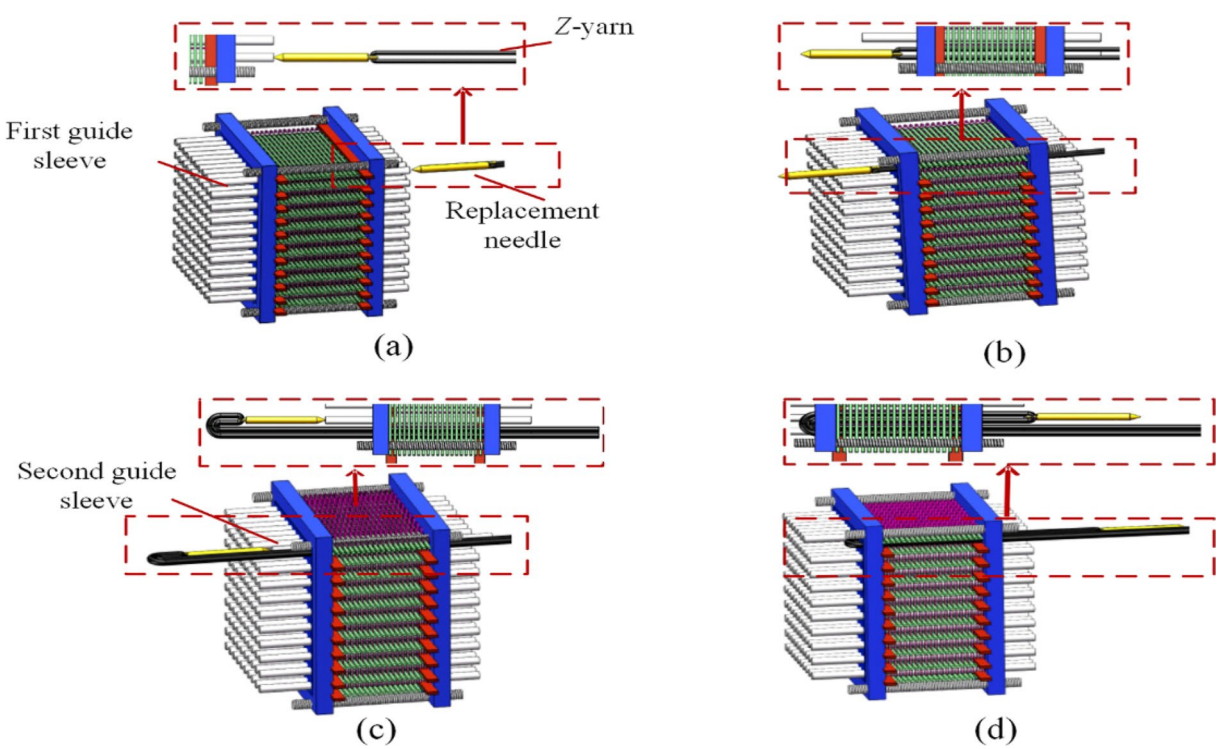

Figure 3 *Z*-yarn replacement guide sleeve

from fiber bundles and metals by observing the friction pattern between bundles and metals. Lee et al. [18] found that damage to carbon fiber bundles during weaving was caused by the guide rods. Archer et al. [19] found that the overall damage caused by weaving of carbon fiber bundles decreased the tensile fracture strength of the bundles by 9%–10%, which is much lower than the performance damage caused by weaving into glass fiber bundles. Sugimoto et al. [20] designed a device to evaluate the dynamic friction between carbon fibers and found that the state of the cladding between the filaments was strongly influenced by compressive stress and had a significant effect on the coefficient of dynamic friction of the fiber.

Current research on fiber friction has revealed the damage mechanism of fibers and studied the fiber wear in the X and Y directions during the weaving process; however, there is no research on the change in damage of Z-yarns after implantation into the precast and on Z-yarn replacement to prevent their breakage in the precast because of high wear.

In this study, we used a homemade tensile-force measuring device to measure preforms of different thicknesses. The force required to replace the guide sleeve at different positions is expressed as F, and is equivalent to the frictional force on the Z-yarn-implanted preform, where the distribution pattern of F is obtained. Modeling the distribution of frictional forces on Z-yarn implantation in preforms with different thicknesses using a back propagation (BP) neural network enables the prediction of frictional forces on large and complex preforms with Z-yarn, and the performing of experiments involving continuous replacement of guide sleeves with Z-yarn for different frictional regions. Via tensile testing, checking the amount of hairiness on the fiber bundle surface, detecting the amount of hairiness on the fiber bundle surface, and the relationship between the wear of Z-yarn in the preform and the number of preform layers, the position of the guide sleeve and the number of replacement guide sleeve were obtained to solve the problem of low preform forming efficiency and poor quality, as shown in Figure 4, to improve the theoretical basis and practical process data for the realization of continuous Z-yarn implantation.

2 Experimental Materials and Methods

2.1 Prefabricated System Preparation

A Toray T300 series 3K carbon fiber tow was selected to complete the weaving of the preform for the flexible-guided three-dimensional structural composite, according to flexible-guided 3D weaving technology.

Guide sleeves were introduced in the thickness direction of the composite preform, which outlined the preform and achieved near-net forming. The guide sleeves lock the fibers woven in layers to provide Z-directional reinforcement. Because the guide sleeves were prepositioned on the weaving guide template, the fibers were woven according to a defined path when the guide sleeves were locked according to a defined locking pattern; therefore, taking maximum advantage of the guide sleeve [21].

The Z-yarn was implanted into the preform after weaving was completed, and the guide sleeves were replaced. On the weaving surface, 3K fiber bundles were wound by 0°/90° guide sleeves in the X and Y directions, respectively, and orthogonal winding was done once; this is defined as weaving into one layer 50, 100, 150, 200, and 250 layers of carbon fiber preforms with thicknesses of 25, 50, 75, 100, and 125 mm, respectively. After weaving, two 6K fiber bundles were implanted into the preform member from the Z direction to complete the in situ replacement of the Z-yarn with the guide sleeves to realize the overall restraint and reinforcement of the preform.

Figure 4 *Z*-yarn implantation condition

2.2 Yarn Replacement Force Measurement Method

A tension-measuring device was designed to replace the guide sleeves and the structural characteristics of the guide sleeves. A gripper was connected to the sensor at one end and to the guide sleeve at the other, and the required replacement force was fed back to the sensor by dragging the guide sleeve outward. The value of the replacement force was displayed on the computer through digital module processing, as shown in Figure 5. Because the weaving process is repetitive and the preform has a rectangular cross-section with axially symmetric characteristics, only 1/4 of the preform cross-section was considered for the study, and each guide sleeve of the preform was taken separately for the yarn replacement force measurement.

Because the tensile force measurement of the replacement guide sleeves included so much data and high volatility factors, the experiment to verify the accuracy of the tensile force measurement was first done on a preform of 50 layers of 25 mm thickness. To ensure the universality of the results, the diagonal position of the guide sleeves was divided into four parts, and five guide sleeves, GS1, GS2, GS3, GS4, and GS5, were taken at the end point for the replacement force measurement. The replacement forces were measured five times for the same guide sleeve, as shown in Figure 6. The maximum error of the yarn replacement force was 5.2%, indicating that the fluctuation and error of the measured yarn replacement force were within the acceptable range and could be used to accurately measure the size of the replacement force of the preform.

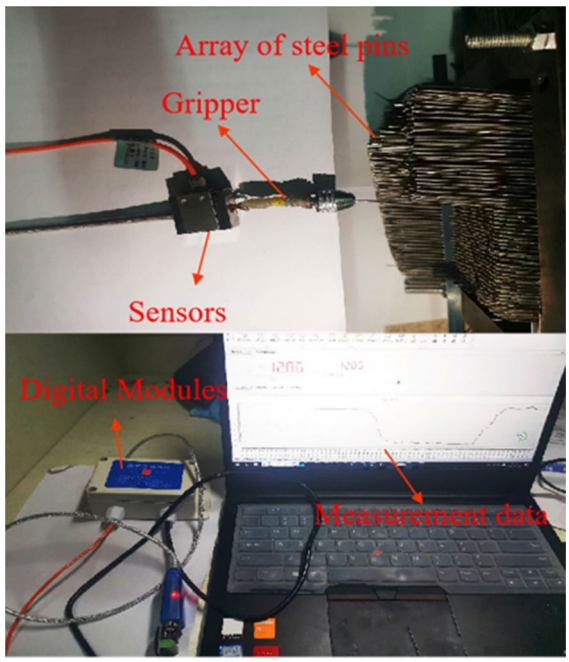

Figure 5 Yarn tying force measurement device

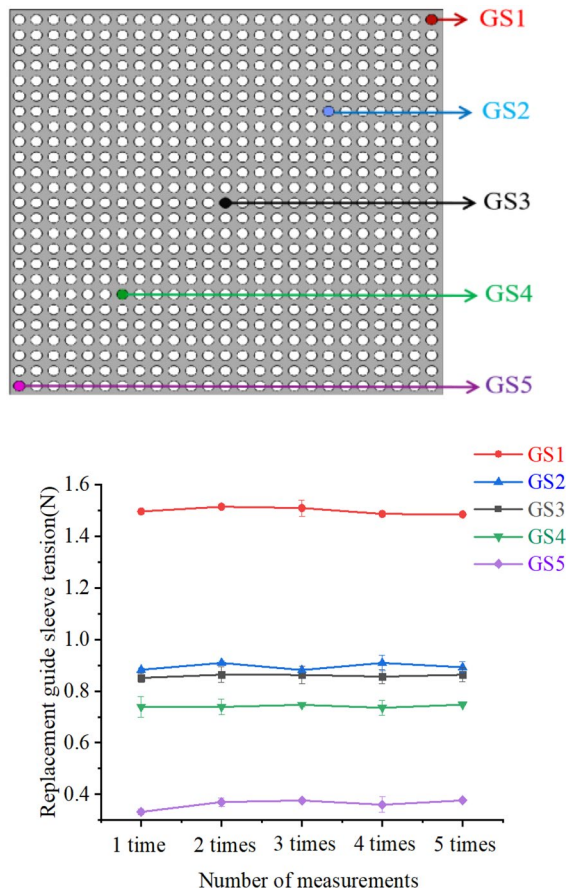

Figure 6 Tensile force measurement of the replacement guide sleeve fluctuations

3 Experimental Results and Analysis

The preform of flexible guided three-dimensional weaving consists of in-plane *X*-direction yarn, in-plane *Y*-direction yarn, and *Z*-directed guide sleeve for *Z*-yarn implantation. The diameter of the guide array was 1.2 mm and the center spacing was 2.4 mm. After the preform was weaved, we used *Z*-yarn to replace the guide sleeves to form a flexible guided three-dimensional woven preform. Liu et al. [21] found that the fiber volume content of the flexible-guided three-dimensional woven preform increased with increasing compressive stress, and the fiber volume fraction changed more rapidly if the preform was compacted when the number of woven layers was small, and the growth trend gradually leveled off as the number of woven layers increased. A higher fiber volume fraction indicates better denseness of the preform, that is, a higher force is required for *Z*-directed guide sleeve replacement. During the compaction process of

the preform, the fiber bundles and guide sleeves squeeze each other to produce small deformations, and the guide sleeves are subjected to different forces at different locations. Therefore, we used the device to measure the replacement force of the guide sleeves at different positions on the preforms of 50, 100, 150, 200 and 250 layers, and the results are shown in Figure 7.

From Figure 7, it can be seen that by measuring the force F required to replace the guide sleeve of the five preforms, the maximum value of the force F required to

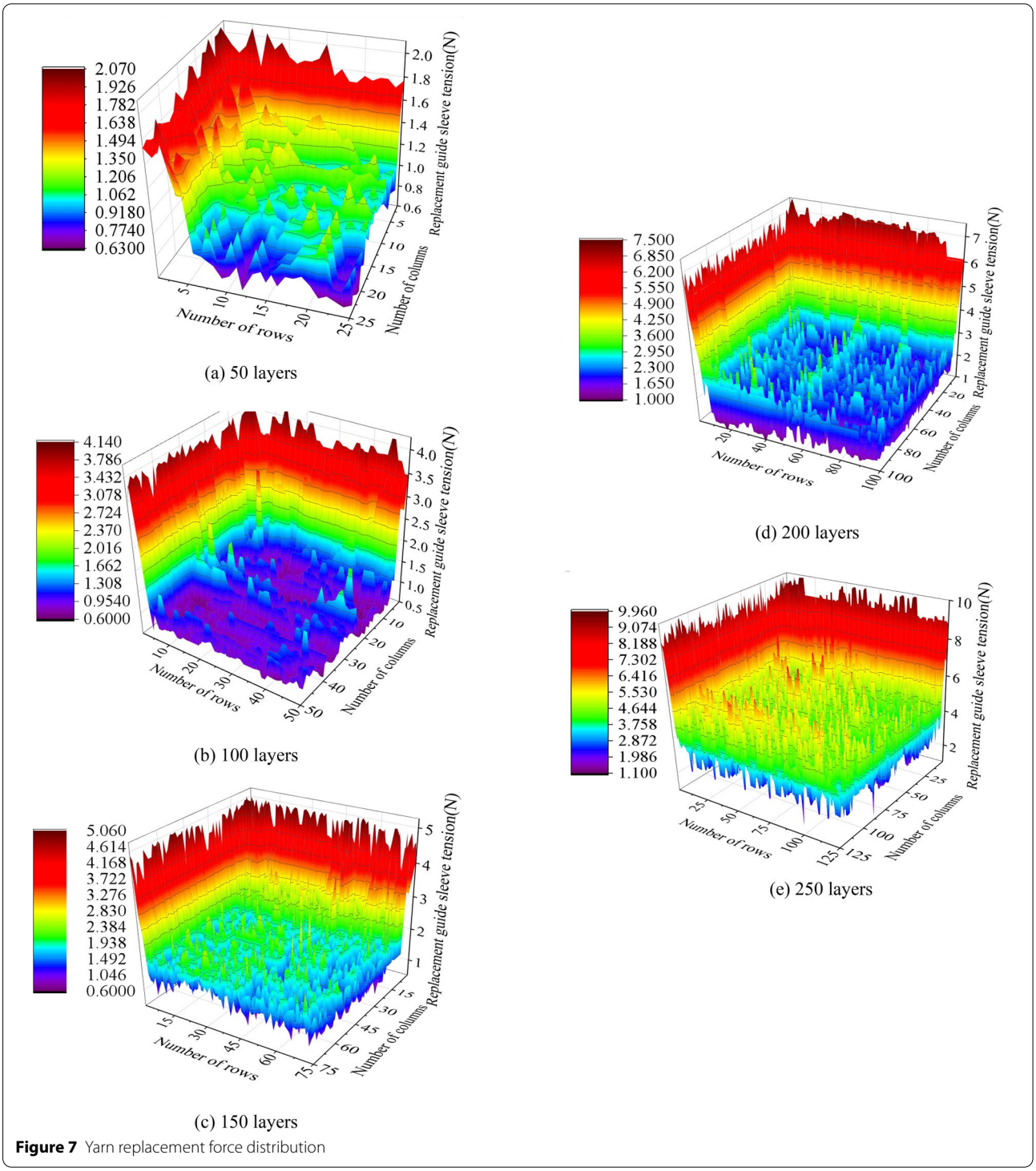

Figure 7 Yarn replacement force distribution

replace the guide sleeve is proportional to the thickness of the fabric; for the same fabric, the F value decreased from the corner, edge, secondary edge, and central part. This is because of the digital flexible guide preform forming process. To ensure the fiber volume fraction of the fabric, it is necessary to apply positive pressure F_1 on the preform; this reduces the height of the preform in the Z direction. Because the volume remains the same, the preform's X and Y direction lengths will increase; however, the guide sleeves limit its displacement in X and Y directions, so the fiber in the X, Y direction will have a force F_2 on the guide sleeves, as shown in Figure 8(a) and (b), resulting in the lowest value of F at the center of the fabric. Therefore, the closer the distance to the outermost guide sleeves, the higher the F value. In addition, after the preform weaving is completed, it must be removed from the table. First, the steel piece is inserted into the gap between the two adjacent rows of the guide sleeve, and the steel piece is inserted into the gap of the pickup frame simultaneously to complete the position of the pickup frame and the fixed preform. Finally, the distance between the two taking frames is adjusted to shift the thickness of the preform to a suitable position, as shown in Figure 8(c). Adjustment of the distance between the pickup frames needs to be completed by the screw, so the corner part of the fabric has the largest deformation of the pickup frame; that is, the outermost corner part of the fabric has the largest force value with the guide sleeves.

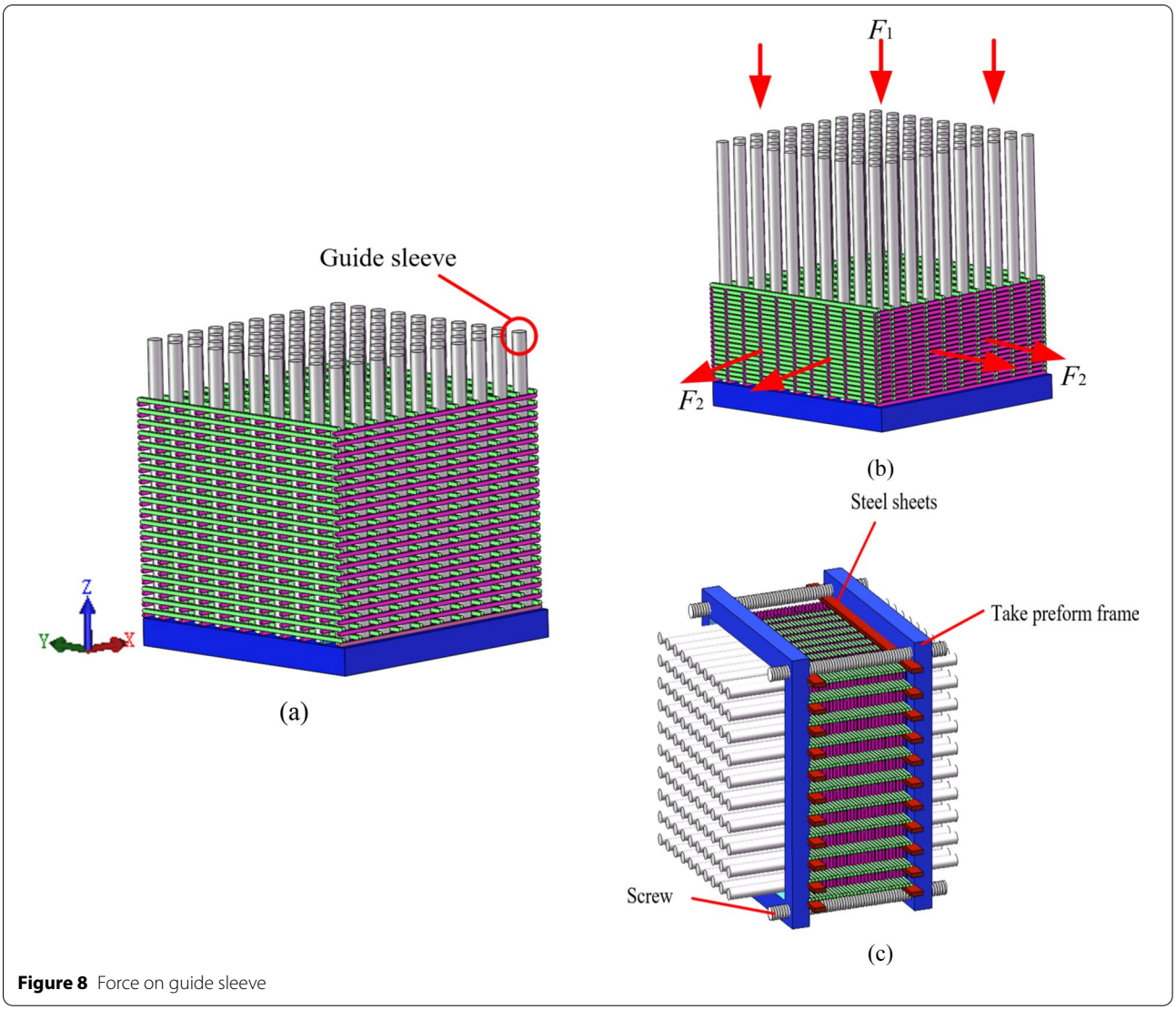

Figure 8 Force on guide sleeve

4 Replacement Yarn Force Distribution Modeling of Preform

Error BP neural networks have a simple structure and can be trained to automatically summarize the functional relationships between data without any a priori formulas; therefore, they have an advantage that traditional mechanical or mathematical methods cannot match [22], and are widely used in financial, biological, medical, health, and marketing research fields [23]. Liu et al. [24] proposed a back-propagation artificial neural network model to predict body dimensions related to pattern making by inputting several key body dimensions. Song et al. [25] found that, compared with a support vector machine (SVM) and random forest (RF), the BP neural network has the best prediction accuracy, generalization ability, and test time. The improved network enhanced the convergence performance, reduced the running time and mean square error. The application of a BP neural network in modeling the replacement force of the preform is important for continuous dynamic prediction of the preform replacement force with different layers at different positions.

4.1 BP Network Modeling

The feedforward network of its learning algorithm was first established, and consisted of an input layer, an implicit layer, and an output layer [26]. The BP learning algorithm consists of two parts: the forward propagation of information and backward propagation of errors. In the forward propagation process, the input information is computed from the input to the output sequentially via the implicit layer, and the state of the neurons in each layer only affects the state of the neurons in the next layer [27]. If the desired output is not obtained at the output layer, the value of the error change at the output layer is calculated and then shifted to backpropagation, where the error signal is backpropagated via the network along the original connection pathway to modify the weights of the neurons in each layer until the desired goal is reached [28]. The configuration of the input layer needs to consider all the elements that affect the output layer, which is the result of the model analysis, i.e., the replacement force. Therefore, for this system, the input layer mainly includes the number of preform layers, the number of array steel needle columns, and the number of array steel needle rows.

The selection of the implied nodes is based on the correct reflection of the input and output, and the number of implied nodes is chosen as rarely as possible, and is gradually increased during training according to the situation until the network performance requirements are met. The initial value of the number of hidden nodes is determined using Eq. (1) [29].

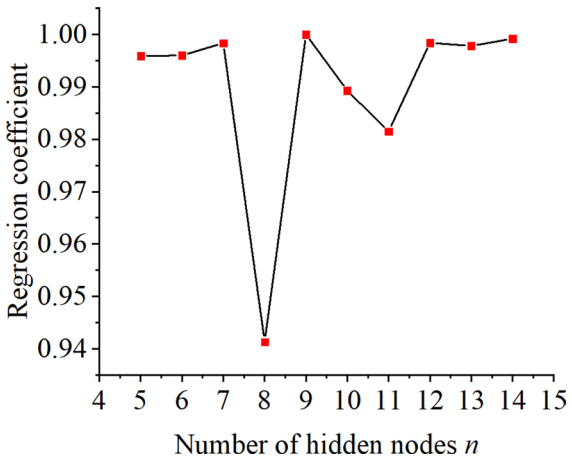

Figure 9 Relationship between hidden nodes and regression coefficients

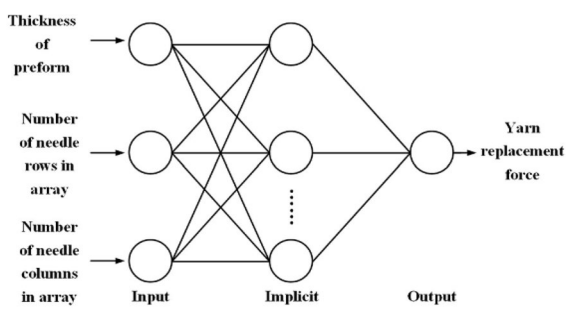

Figure 10 BP neural network model for cutting force prediction

$$n = \sqrt{n_i + n_0} + a, \tag{1}$$

where n is the number of hidden layer nodes, n_i is the number of input nodes, n_0 is the number of output nodes, and a is a constant between one and ten.

In this study, the implicit nodes were initially selected among 5–14 according to the smallest possible value of the number of input and output nodes. The network was trained for different implicit layers, and an analysis of the predicted regression coefficient was conducted. The regression against the number of hidden nodes n is shown in Figure 9. The more the regression coefficient tends to 1, the better the fitting effect; therefore, the best implicit layer node number was finally selected as 9.

The structure of the feedforward neural network is shown in Figure 10.

MATLAB provides a variety of improved neural network tool functions, and this study utilizes the fast

Table 1 Comparison of the effect of different BP training

Training algorithms	Mean Square Error		
	Training	Validation	Testing
Levenberg-Marquardt	$2.244e^{-4}$	$2.708e^{-2}$	$2.706e^{-2}$
Bayesian Regularization	$5.431e^{-4}$	$7.2553e^{-4}$	$6.954e^{-4}$
Scaled Conjugate Gradient	$5.617e^{-1}$	$1.897e^{-1}$	$1.514e^{0}$

BP algorithm, which is a method that uses a combination of momentum and adaptive learning rate to train the forward network. BP algorithms mainly include the Levenberg-Marquardt algorithm, Bayesian regularization algorithm, Scaled conjugate gradient algorithm, and other selected algorithms under the same conditions for training the network. The results are compared and analyzed, and the mean square error is used as the criterion for algorithm selection, as shown in Table 1.

According to the run results, the Bayesian regularization algorithm has the smallest mean square error and is the most stable; therefore, it was chosen as the training algorithm for the replacement yarn force distribution model.

When designing a BP neural network, it is necessary to determine the topology of the network (the number of layers of the hidden layers and the number of neurons in each layer), the transformation function of its neurons, initialization of the network, error calculation, learning rules and network training, training parameters, and normalization of training samples. The MATLAB Neural Net Fitting Tool includes important excitation functions, such as nonlinear functions and the sigmoid linear function type used in this study. The neural network structure, number of neurons set, according to their own needs to call the neural network in the toolbox, modify the network connection weights and threshold rules, and write a variety of network training procedures to achieve a variety of desired functions [30].

4.2 Network Training and Result Analysis

The neural network training for the replacement yarn model consists of three main neuronal inputs: x_1 is the number of preform layers, x_2 is the number of rows of array stitches, and x_3 is number of columns of array stitches; these are connected to the three weights (w_1, w_2, and w_3) of the weight adjustment inputs weighting ratio. Selecting the most efficient linear weighted summation yields the $\mathrm{Net_{in}}$ neuron net input Eq. (2).

$$Net_{in} = \sum_{i=1}^{n} w_i x_i. \tag{2}$$

The activation function was chosen as the Sigmoid function which transforms the input from negative infinity to positive infinity with an output between 0 and 1. If there is no constraint, a linear activation function (the sum of the multiplication of the weights) can be used, yielding the output of Eq. (3).

$$y = \mathrm{sigmoid}\left(\sum_{i=1}^{n} w_i x_i\right). \tag{3}$$

The Sigmoid function is defined as Eq. (4).

$$\mathrm{sigmoid}(x) = \frac{1}{1+e^{-x}}. \tag{4}$$

Substituting Eq. (4) into Eq. (3) yields Eq. (5).

$$y = \frac{1}{1+e^{-Net_{in}}}. \tag{5}$$

A logical model of the training threshold for the substitution force network is shown in Figure 11.

As shown in Figure 10, the three nodes in the input layer are numbered 1, 2, and 3, and the hidden layer has nine nodes, numbered 4–12, and the output layer has one node, numbered 13. The data were analyzed using the yarn force data of different positions using 50, 100 and 150 layers of preforms as samples, and the input and output matrices were established as 222 × 75 and 1 × 75, respectively. According to the values of nodes 1, 2 and 3 from Eq. (3), the output values of node 4 can be obtained using Eq. (6).

$$\begin{aligned} a_4 &= \mathrm{sigmoid}\left(\sum_{i=1}^{n} \mathrm{w_i} x_i\right) \\ &= \mathrm{sigmoid}(w_{41}x_1 + w_{42}x_2 + w_{43}x_3). \end{aligned} \tag{6}$$

where w_{41}, w_{42} and w_{43} are the weights of nodes 1, 2, and 3 relative to node 4, respectively, and the output values of nodes 5 to 12 can be calculated; therefore, nine values of the hidden nodes can be calculated. The network input

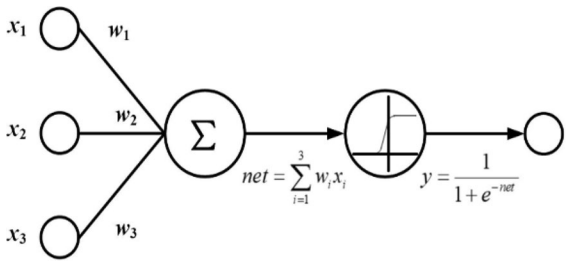

Figure 11 Sigmoid threshold unit model

vector and weight vector of each node in the hidden layer are defined as follows:

$$\boldsymbol{x} = \begin{bmatrix} x_1 \\ x_2 \\ x_3 \\ 1 \end{bmatrix}, \tag{7}$$

$$\boldsymbol{W} = \begin{bmatrix} \boldsymbol{w}_4 \\ \boldsymbol{w}_5 \\ \boldsymbol{w}_6 \\ \vdots \\ \boldsymbol{w}_{12} \end{bmatrix} = \begin{bmatrix} w_{41}, w_{42}, w_{43} \\ w_{51}, w_{52}, w_{53} \\ w_{61}, w_{62}, w_{63} \\ \vdots \\ w_{121}, w_{122}, w_{123} \end{bmatrix}, \tag{8}$$

$$\boldsymbol{a} = \begin{bmatrix} a_4 \\ a_5 \\ a_6 \\ \vdots \\ a_{12} \end{bmatrix}. \tag{9}$$

Combining Eqs. (6)– (9) yields Eq. (10).

$$\boldsymbol{a} = \text{sigmoid}(\boldsymbol{W} \bullet x). \tag{10}$$

Because the algorithm of each layer is the same, for the alternative yarn force distribution network model with three input nodes, one output layer, and nine hidden layers, we assume that the weight matrices are $\boldsymbol{w_1}$, $\boldsymbol{w_2}$, $\boldsymbol{w_3}$,…,$\boldsymbol{w_{12}}$, each hidden output is $\boldsymbol{a_1}$,$\boldsymbol{a_2}$, $\boldsymbol{a_3}$,…,$\boldsymbol{a_{11}}$, the input of the neural network is $\boldsymbol{x}$ and the output of the neural network is y, then the output vector of each layer can be computed and expressed as Eq. (11).

$$\begin{cases} \boldsymbol{a}_1 = \text{sigmoid}(\boldsymbol{w}_1 \bullet \boldsymbol{x}), \\ \boldsymbol{a}_2 = \text{sigmoid}(\boldsymbol{w}_2 \bullet \boldsymbol{a}_1), \\ \boldsymbol{a}_3 = \text{sigmoid}(\boldsymbol{w}_3 \bullet \boldsymbol{a}_2), \\ \vdots \\ y = \text{sigmoid}(\boldsymbol{w}_{12} \bullet \boldsymbol{a}_{11}). \end{cases} \tag{11}$$

Then, the input data are normalized using the Mapminmax function to obtain the input and output, and the normalization function is presented as in Eq. (12).

$$y' = 2\frac{x_n - x_{\min}}{x_{\max} - x_{\min}} - 1. \tag{12}$$

The inverse normalization function is presented in Eq. (13).

$$x_n = y' \bullet (x_{\max} - x_{\min}) + x_{\min}, \tag{13}$$

where x_n is the nth input data, $x_{\max}$ is the maximum value of the input data, $x_{\min}$ is the minimum value of the input data, and y' is the nth normalized data. After the results are obtained and then reverse-normalized to determine the magnitude of the yarn replacement force at different positions, the fit of the test sample is shown in Figure 12.

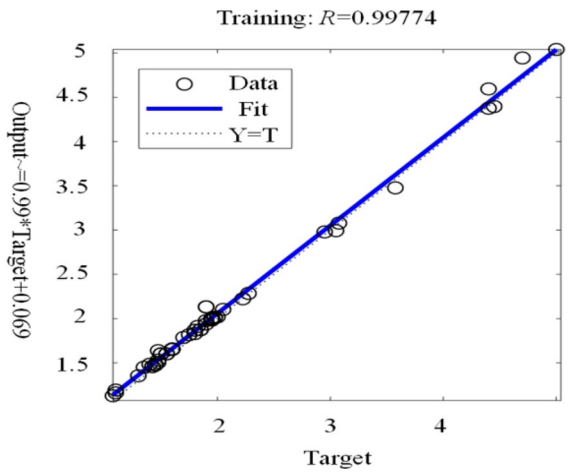

Figure 12 Bayesian network training sample fit

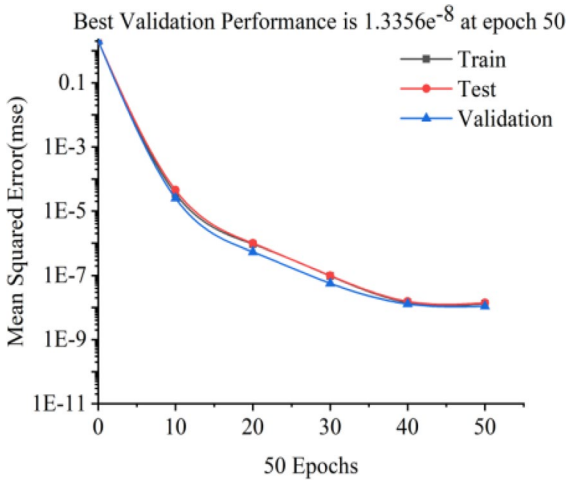

Figure 13 Neural network Performance fit

The mean square error of the training set, validation set, test set, and overall, with the number of trainings is shown in Figure 13.

It can be seen that the accuracy of this fitting is very high, and the training was completed 50 times with a mean square error of $1.3356e^{-8}$, without overfitting. After establishing the replacement force distribution model, the neural network function (x) in MATLAB was used to predict the required replacement force magnitude by inputting the number of preform layers, number of steel array pin rows, and the number

of steel array pin columns in X-direction, respectively, into the actual value of the neural network. To further verify the accuracy of the model, the values of the yarn replacement force were predicted for 200 and 250 layers preforms with different number of rows and columns, respectively. The errors between the predicted and actual values for different guide sleeve positions are shown in Figure 14.

The above results show that the simulated value of the BP network model for predicting the yarn replacement force fits well with the actual value, and the more the preform layers, the greater the yarn replacement force, and the better the fitting effect. The maximum error is 1.9%, which is of great practical significance in determining the size of the yarn replacement force at different layers and different positions of the preform.

5 *Z*-yarn Strength Factor Analysis

The shear resistance of carbon fiber is poor, and it is easy to cause wear of carbon fiber in the process of implanting the preform. This shows that the fiber surface is rough or even broken, which will lead to an interruption in the continuous implantation of carbon fiber, reduce the forming efficiency of the preform, decrease the volume fraction of Z-yarn in the preform, and greatly affect the overall mechanical properties of the preform.

Combining these results with the prediction model of the yarn replacement force distribution derived from the previous section, we selected the 150 layers preform as the experimental object. Also, six positions with replacement forces of 1.75, 2, 2.5, 3, 3.5 and 4 N were selected to replace the guide sleeves 5, 10, 15, 20, and 25 times with two 6 K carbon fiber bundles from Toray, Japan, as the Z-yarn. The replacement speed was 5 mm/s, and the Z-yarn movement distance was 75 mm. The Z-yarn was glued to a reinforcement piece of 50 mm in length and 10 mm in width, and the length of fiber between the reinforcement pieces was 150 mm. The maximum breaking strength of the Z-yarn under different replacement times was tested using a universal tensile testing machine with a loading speed of 2 mm/min, as shown in Figure 15.

The relationship between the number of different fiber replacements and fiber breaking strength of the Z-yarn in the same area of the preform was obtained, as shown in Figure 16(a); for the same number of replacements, the relationship between different position areas and fiber breaking strength was obtained, as shown in Figure 16(b).

From Figure 16(a), it can be seen that for the same preform area, as the number of yarn replacements of the guide sleeves increases, the breaking strength of the fiber becomes smaller. From Figure 16(b), it can be seen that the greater the frictional force on the fiber in the Z direction, the more obvious the decrease in the breaking strength of the fibers as the number of replacements increases. In the area where the friction force was 4 N, the replacement force of the Z-yarn implanted 25 times decreased substantially. The surface morphology of the

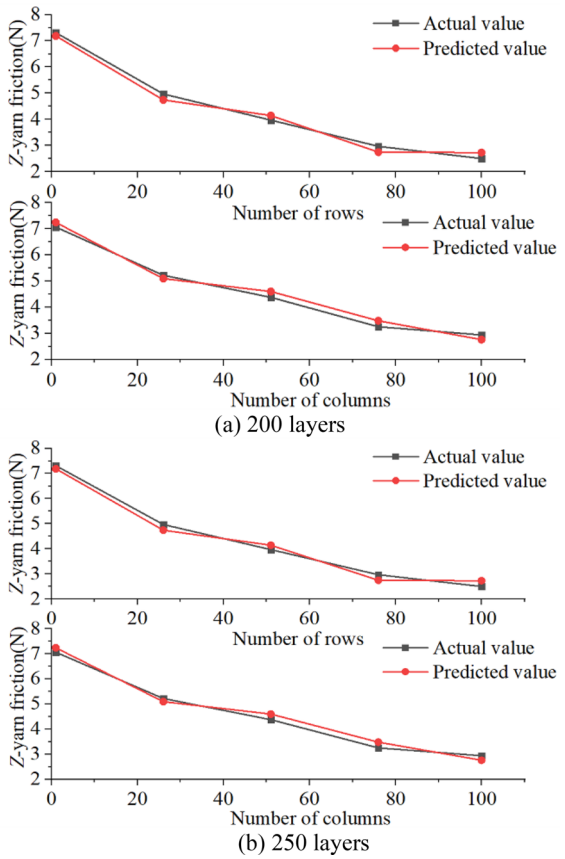

Figure 14 Fitting of preform with different layers and different positions

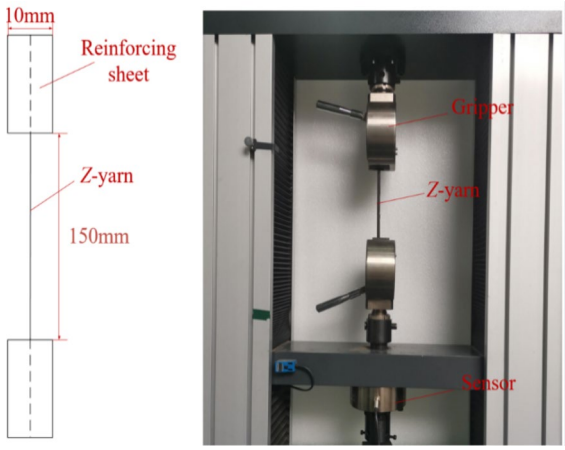

Figure 15 Z-yarn tensile strength test

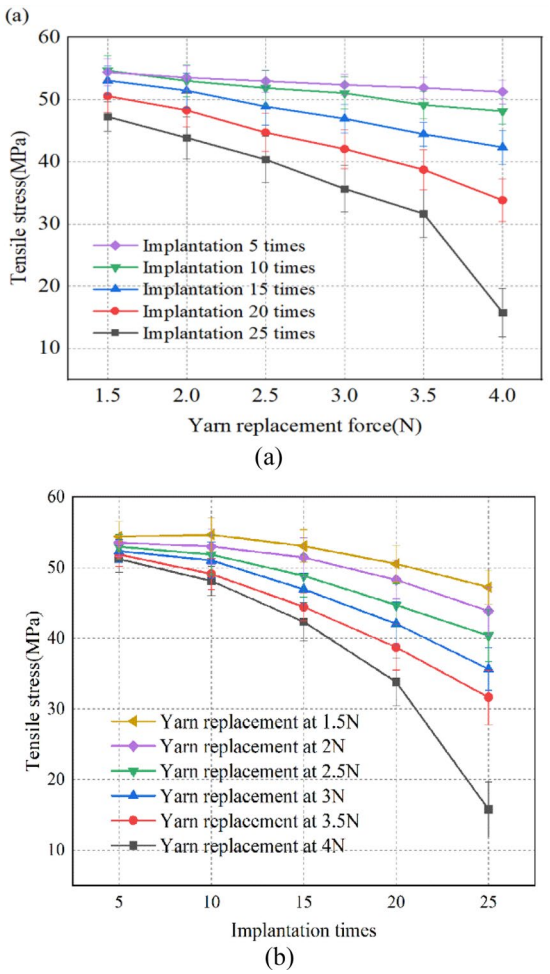

Figure 16 Fiber fracture strength as a function of preform position and friction number

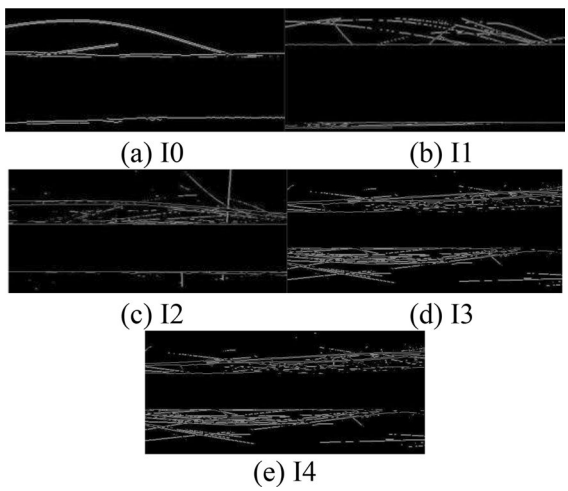

Figure 17 Z-yarn surface hairiness at different implantation times

Z-yarn with different implantation times is shown in Figure 17. The hairiness area of the upper and lower parts of the dimensional bundle were selected, and the average grayness value of the area was calculated; the greater the amount of hairiness, the greater the grayness value, and the more severe the fiber wear [31].

From Figure 17(a), it can be seen that the surface of the carbon fiber bundle is relatively smooth when the number of implantations is 5; with an increase in the number of implantations, as shown in Figures 17(b)–(e), the number of hairiness produced on carbon fiber bundle surface also increases. This is because the more the number of implantations, the more frequent the mutual friction between the fibers inside the *Z*-yarn bundle and the *X* and *Y*-directional fibers in the preform, which causes a certain amount of hairiness on the surface of the carbon fiber bundle. Table 2 shows the statistics on grayscale values of hairiness in samples with different *Z*-yarn implantations. It can be seen that the amount of hairiness in sample I4 is the highest, followed by that of sample I3, and the amount of hairiness in sample I0 is the least; from the perspective of friction, the more hairiness, the more damage the carbon fiber bundle suffers, and this is consistent with the variation in tensile properties.

Therefore, to avoid yarn breakage in the preform, which affects the strength of the *Z*-yarn, it is necessary to replace the guide sleeve 20–25 times in the corner position of the preform, that is, when the *Z*-yarn is implanted in the preform at a distance of 1500–1875 mm, the *Z*-yarn needs to be replaced in time.

6 Conclusions

(1) The designed tensile force measuring device and sensors were used to accurately measure the size of the replacement force at different positions for 50, 100, 150, 200 and 250 layers of carbon fiber preforms, revealing that the size of the replacement force of the carbon fiber preforms decreases from the corner, edge, secondary edge and central part in order.

(2) The number of preform layers and the number of guide sleeve rows and columns were used as input layers, and the replacement force was used as the output layer. Different algorithms were compared,

Table 2 Statistics of hairy gray value of *Z*-yarn samples under different implantation times

Serial number	I0	I1	I2	I3	I4
Number of implantation	5	10	15	20	25
Grayscale value	96.203	97.510	98.424	99.543	101.862

the optimal genetic algorithm was selected for the 150-layer preform yarn force data, and a model was developed to predict the distribution of replacement forces at different positions for preforms with different number of layers. The predicted value was within 1.9% of the actual error, effectively predicting the distribution of preform friction for different thicknesses and number of layers.

(3) As the number of guide sleeve replacements increases in the *Z*-yarn, the tensile fracture strength of carbon fiber bundles decreases, and the amount of hair and feathers gradually increases, indicating a gradual increase in wear and tear. At the middle and the sub-edge positions of the preform, the *Z*-yarn tensile breaking strength loss is not significantly affected by the number of guide sleeve replacements. At the edge of the preform, the loss of *Z*-yarn tensile strength at break is influenced by the number of guide sleeve replacements with a significant linear decreasing trend. At the corner position of the preform, there is a significant nonlinear decrease in fiber tensile breaking strength. To avoid fiber breakage during implantation, when the *Z*-yarn is replaced in the corner 20–25 times, the *Z*-yarn needs to be replaced in time.

Acknowledgements
Not applicable.

Author contributions
ZS was in charge of the whole trial; ZG wrote the manuscript; JH and DX assisted with sampling and laboratory analyses. All authors read and approved the final manuscript.

Authors' Information
Zitong Guo, born in 1991, is currently a graduate student jointly trained by *University of Science and Technology Beijing* and *China Academy of Machinery Sciences and Technology Group*. His research direction is digital flexible guided 3D weaving preform forming Tel: 18810611586
Zhongde Shan, born in 1970, is currently the president of *Nanjing University of Aeronautics and Astronautics*. His research is the development of advanced manufacturing technology and electromechanical equipment, energy conservation and emission reduction of machinery industry and green manufacturing research.
Jihua Huang, born in 1962, is currently a professor at *University of Science and Technology Beijing*. His research direction is advanced materials and dissimilar material connection.
Debo Xue, born in 1987, is currently a graduate student at *Shandong University of Technology*. His research direction is carbon fiber preform weaving.

Funding
Supported by the National Defense Basic Scientific Research Program of China (Grant No. 2017-JCJQ-ZD-035) and National Natural Science Foundation of China (Grant No. 51790173).

Competing Interests
The authors declare no competing financial interests.

Author Details
[1]School of Materials Science and Engineering, University of Science and Technology Beijing, Beijing 100083, China. [2]Nanjing University of Aeronautics and Astronautics, Nanjing 210016, China. [3]State Key Laboratory of Advanced Forming Technology and Equipment, China Academy of Machinery Science and Technology Group Co. ltd, Beijing 100083, China. [4]School of Mechanical Engineering, Shandong University of Technology, Zibo 255000, China.

Received: 28 November 2021 Revised: 10 March 2022 Accepted: 25 March 2022
Published online: 02 June 2022

References

[1] Xiaofei Zhu, Yulei Zhang, Jian Zhang, et al. A gradient composite coating to protect SiC-coated C/C composites against oxidation at mid and high temperature for long-life service. *Journal of the European Ceramic Society*, 2021, 41(16): 123-131.
[2] A Lazzari, D Tonazzi, J Brunetti, et al. Contact instability identification by phase shift on C/C friction materials. *Mechanical Systems and Signal Processing*, 2022, 171: 108902.
[3] Fei Lu, Jian Liu, Hongyan Lu. Experimental study on leakage and wear characteristics of C/C composite finger seal. *Industrial Lubrication and Tribology,* 2020, 72(10): 1133–1138.
[4] R Djugum, K Sharp. The fabrication and performance of C/C composites impregnated with TaC filler. *Carbon*, 2017, 115: 105-115.
[5] V Gamaleev, Oh Jun-Seok, H Furuta, et al. Investigation of effect of needle electrode configuration on microplasma discharge process in sea water. *IEEE Transactions on Plasma Science*, 2017, 45(4): 754–760.
[6] M Jabbar, K Shaker, Y Nawab, et al. Effect of the stuffer yarns on the mechanical performance of Novel 3D woven green composites. *Composite Structures*, 2021, 269(1):114023.
[7] Li Chen, Wei Jiao, Xinmiao Wang, et al. Progress in the study of mechanical properties of three-dimensional woven composites. *Materials Engineering*, 2020, 48(8): 62-72. (in Chinese)
[8] Zhongde Shan, Li Zhan, Yunliang Miao, et al. Digital precision forming technology and equipment for composite components. *Science and Technology Herald*, 2020, 38(14): 63-67. (in Chinese)
[9] Hassan M ElDessouky, Mohamed Nasr Saleh, Ying Wang. Effect of unit-cell size on the barely visible impact damage in woven composites. *Applied Sciences*, 2021, 11(5): 2364.
[10] Midani Mohamad, Seyam Abdel-Fattah, Saleh Mohamed Nasr, et al. The effect of the through-thickness yarn component on the in and out-of-plane properties of composites from 3D orthogonal woven preforms. *The Journal of The Textile Institute*, 2019, 110(3): 317-327.
[11] M Esmaeeli, M R Nami, B Kazemianfar. Geometric analysis and constrained optimization of woven z-pinned composites for maximization of elastic properties. *Composite Structures*, 2019, 210(Feb.): 553-566.
[12] K Bilisik. Dimensional stability of multiaxis 3D-woven carbon preforms. *The Journal of The Textile Institute*, 2010, 101(5): 380-388.
[13] Huajie Xu, Litong Zhang, Laifei Cheng. Effects of yarn size and Z-yarn density on the interlaminar shear properties of two Z-reinforced 3D C/SiC composites. *Materials and Design*, 2014, 64: 434-440.
[14] G H Eddine, G Barbier, C W Kocher, et al. Experimental evaluation of transverse friction between fibers. *Tribology International*, 2018, 119: 112-122.
[15] S Allaoui, G Hivet, A Wendling, et al. Influence of the dry woven fabrics meso-structure on fabric/fabric contact behavior. *Journal of Composite Materials*, 2012, 46(6): 627-639.
[16] M Tourlonias, M A Bueno, C Jordan, et al. Influence of wear on the sizing layer and desizing of single carbon fibre to fibre friction. *Wear*, 2018, 402: 64-70.
[17] B Cornelissen, U Sachs, B Rietman, et al. Dry friction characterisation of carbon fibre tow and satin weave fabric for composite applications. *Composites Part A: Applied Science and Manufacturing*, 2014, 56: 127-135.
[18] B Lee, K H Leong, I Herszberu. Effect of weaving on the tensile properties of carbon fiber tows and woven composites. *Journal of Reinforced Plastics & Composites*, 2001, 20(8): 652-670.
[19] E Archer, S Buchanan, A Mcilhaulier, et al. The effect of 3D weaving and consolidation on carbon fiber tows, fabrics, and composites. *Journal of Reinforced Plastics and Composites*, 2010, 29(16): 3162-3170.
[20] Yoshiki Sugimoto, Daisuke Shimamoto, Yuji Hotta. Evaluation of kinetic friction coefficients between single carbon fibers. *Carbon*, 2020, 167: 264-269

[21] Yunzhi Liu, Li Zhan, Zheng Wang, et al. Microstructure analysis of flexible guided 3D woven composite preform. *Progress in Materials in China*, 2020, 39(6): 458–463. (in Chinese)
[22] Li Zhang, Fulin Wang, Ting Sun, et al. A constrained optimization method based on BP neural network. *Neural Computing and Applications*, 2018, 29(2): 413-421.
[23] Dongyao Jia, Chuanwang Zhang, Dandan Lv. Evaluation of road condition based on BA-BP algorithm. *Journal of Intelligent & Fuzzy Systems*, 2020, 40(1): 331-348.
[24] Kaixuan Liu, Jianping Wang, Edwin Kamalha, et al. Construction of a prediction model for body dimensions used in garment pattern making based on anthropometric data learning. *The Journal of The Textile Institute*, 2017, 108(12): 2017-2114.
[25] Shaohui Song, Xingyu Xiong, Xin Wu, et al. Modeling the SOFC by BP neural network algorithm. *International Journal of Hydrogen Energy*, 2021, 46(38): 20065-20077.
[26] Haoqi Li, Baucom B, Georgiou P. Linking emotions to behaviors through deep transfer learning. *Peer J Computer Science*, 2020, 6(2): e246.
[27] S D Lee, C H Jun. Fast incremental learning of logistic model tree using least angle regression. *Expert Systems with Applications*, 2018(97): 137-145.
[28] S Panda, G Panda. Performance evaluation of a new BP algorithm for a modified artificial neural network. *Neural Processing Letters*, 2020, 51(4): 1869–1889.
[29] Biao Wang, Feifei Qin, Xiaobo Zhao, et al. Equalization of series connected lithium-ion batteries based on back propagation neural network and fuzzy logic control. *International Journal of Energy Research*, 2020, 44(6): 4812-4826.
[30] Xiaolin Li, Peng Wang, Xinjian Xu, et al. Universal behavior of the linear threshold model on weighted networks. *Journal of Parallel and Distributed Computing*, 2019, 123: 223-229.
[31] M A Bueno, B Durand, Renner M. Optical characterization of the state of fabric surfaces. *Optical Engineering*, 2000, 39(6): 1697.